Polar Geosci., **17**, 139–155, 2004

Features of seismic waves recorded by seismic exploration in 2002: Responses from valley structure of the bedrock beneath Mizuho Plateau

Akira Yamada[1]*, Masaki Kanao[2] and Mikiya Yamashita[3]

[1] *Geodynamics Research Center, Ehime University, Bunkyo-cho 2–5, Matsuyama 790-8577*
[2] *National Institute of Polar Research, Kaga 1-chome, Itabashi-ku, Tokyo 173-8515*
[3] *Department of Polar Science, The Graduate University for Advanced Studies, Kaga 1-chome, Itabashi-ku, Tokyo 173-8515*
**Corresponding author. E-mail: yamada@sci.ehime-u.ac.jp*

(Received April 2, 2004; Accepted June 21, 2004)

Abstract: Seismic waves from natural sources were recorded in seismic exploration experiments in January 2002 by the 43rd Japanese Antarctic Research Expedition (JARE-43). Three kinds of seismic waves were recorded: (1) a teleseismic event occurred in the Kermadec Is. region, (2) local icequakes and (3) an unidentified event. The teleseismic waves show high signal-to-noise ratio in spite of the small magnitude of the event: this indicates that it is highly feasible to study not only the local shallow structure but also the deep structure of the earth by using teleseismic events. Frequency spectra of the waveforms show discordances along the observation line. The 2.0 Hz frequency component is very small in waveforms recorded by stations in the middle part of the observation line. On the other hand, the 1.5, 3.0 and 5.0 Hz frequency components are large in the records of these stations. These stations are located just above the valley topography of the interface between the ice sheet and the upper crust, which has been revealed by JARE-41 and JARE-43 seismological experiments.

key words: Mizuho Plateau, seismic waveforms, stacking, frequency content, valley structure

1. Introduction

Seismic exploration experiments were performed during the 43rd Japanese Antarctic Research Expedition (hereafter JARE-43) in the austral summer season of 2001–2002. These formed part of the "Structure and Evolution of the East Antarctic Lithosphere (SEAL)" project (Kanao, 2001) on the structure of the crust and upper mantle beneath the Mizuho Plateau, East Antarctica (Fig. 1). The JARE-43 experiments recorded seismological data from seven large explosions with 161 temporary seismic stations (for a detailed explanation of the experiments, see Miyamachi *et al*., 2003a). Miyamachi *et al*. (2003b) determined a *P*-velocity structure from the surface to a depth of about 50 km along the JARE-43 line by analyzing first arrival data with a refraction method.

One interesting feature in the structure obtained above is the existence of complex

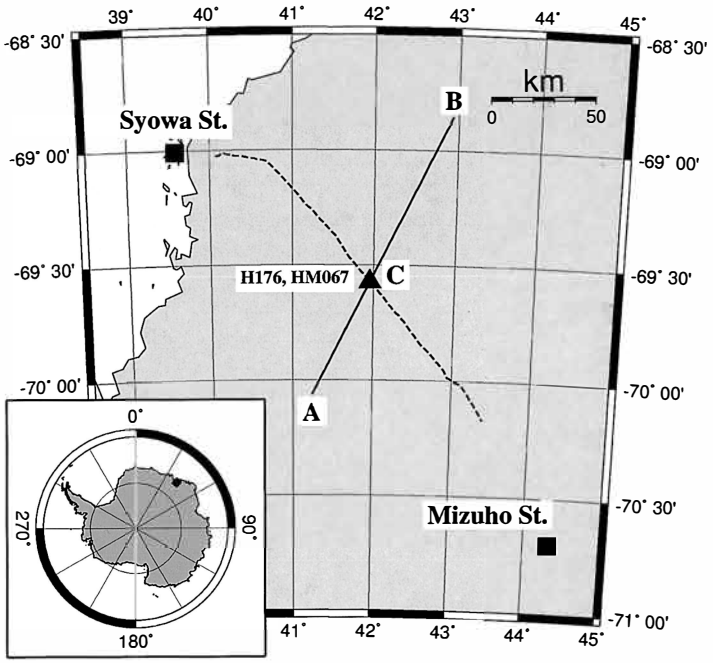

Fig. 1. Map of the observation lines of JARE-43 (solid line) and JARE-41 (broken line) seismic experiments. The station at the intersection of the two seismic lines is indicated by a solid triangle. H176 and HM067 are station codes of JARE-41 and JARE-43, respectively. Positions of A, B and C correspond to those in Fig. 2. The distance measured from A along the JARE-43 line is used as the abscissa (Figs. 2–5, 7a, 8, 10 and 12) and the ordinate (Fig. 6). The study area in Antarctica is indicated by the solid rectangle shown at the lower left.

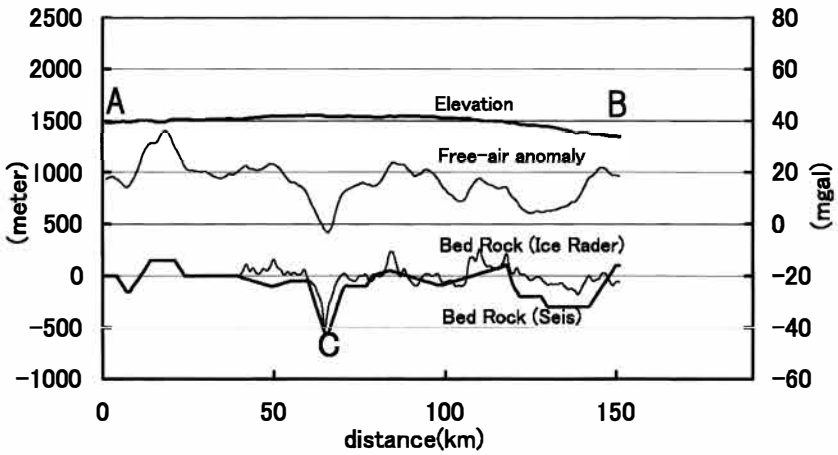

Fig. 2. Comparison of geophysical observations along the line A-C-B in Fig. 1; elevation of the ice surface (scale on the left side), free-air anomaly (scale on the right side) (Toda et al., 2003), depth to the bedrock inferred from radio echo soundings (Takada et al., 2003) and seismic travel-time analysis (Miyamachi et al., 2003b). A, B and C show the locations of points A, B and C in Fig. 1.

topography in the boundary between the ice sheet and the upper crust (Fig. 2). This topography shows (1) a valley structure beneath the stations at a distance of about 65 km (C in Fig. 2) with a width of about 10 km and a depth of 500 m below sea level: (2) a trough beneath the stations in a distance range of about 120–150 km. The valley structure is also found by radio echo sounding by JARE-43 along the same experiment line (Takada *et al*., 2003). This anomalous feature has already been recognized in a seismic survey conducted by JARE-41 (Miyamachi *et al*., 2001; Tsutsui *et al*., 2001). The observation line in JARE-41 was almost perpendicular to that in JARE-43 (Fig. 1); the valley structure is just beneath the intersection of the two lines. Takada *et al*. (2003) pointed out a possibility that water would fill the valley (Mae, 1978), as many subglacial lakes have been reported in the Antarctic (*e.g.* Kapitsa *et al*., 1996; Siegert *et al*., 2001). The *P* velocities beneath these strange depressions, which were determined by Miyamachi *et al*. (2003b), were estimated to be slower (6.05 and 5.90 km/s, just beneath the valley and the trough, respectively) than those in other areas (6.07–6.15 km/s). This might suggest the existence of water within the valley.

Seismic waves caused by natural sources (regional and teleseismic events and local icequakes) were recorded in JARE-43 seismic experiment data, though the recording time-length of the data loggers was limited to only several minutes a day during the experiment. We will show several remarkable features of the anomalies in travel times, amplitudes and frequency spectra in three examples of recorded waveforms from natural sources. Then we will explain the origin of these interesting features in terms of wave propagation across the local heterogeneous structure such as valley topography beneath the Mizuho Plateau.

2. Data

161 seismographs of the vertical component with a natural period of 0.5 s were aligned on the JARE-43 seismic line (Fig. 1) with an interval of 1 km (0.5 km for a 10 km span in the middle part of the line). Recordings with duration of seven and half minutes were performed twice a day (1400 and 1600 in UTC) during the experiments from Jan. 8 to 27, 2002 (Miyamachi *et al*., 2003a). In spite of the short recording time, several kinds of seismic phases were identified and are classified into three types as shown below.

2.1. Kermadec Is. event

Figure 3 shows a teleseismic event from the Kermadec Is. region (Jan. 21, 2002, 1350:58.8 (UTC); event locations are 179.633° E, 31.255° S, 437 km depth and 4.5 m_b). The epicentral distance from this event to the JARE-43 seismic line is about 75°. The direct *P* signal can be clearly and coherently seen throughout the observation line in spite of the small magnitude of the earthquake. This high signal-to-noise ratio shows the success of the high-sensitivity seismic observation on the Mizuho Plateau, which helps us to investigate not only the local structure just beneath the observation line but also the deep interior of the earth.

These teleseismic signals have a sufficient correlation of waveforms among seismic stations and have frequency components lower than 2.0 Hz due to long-path propagation

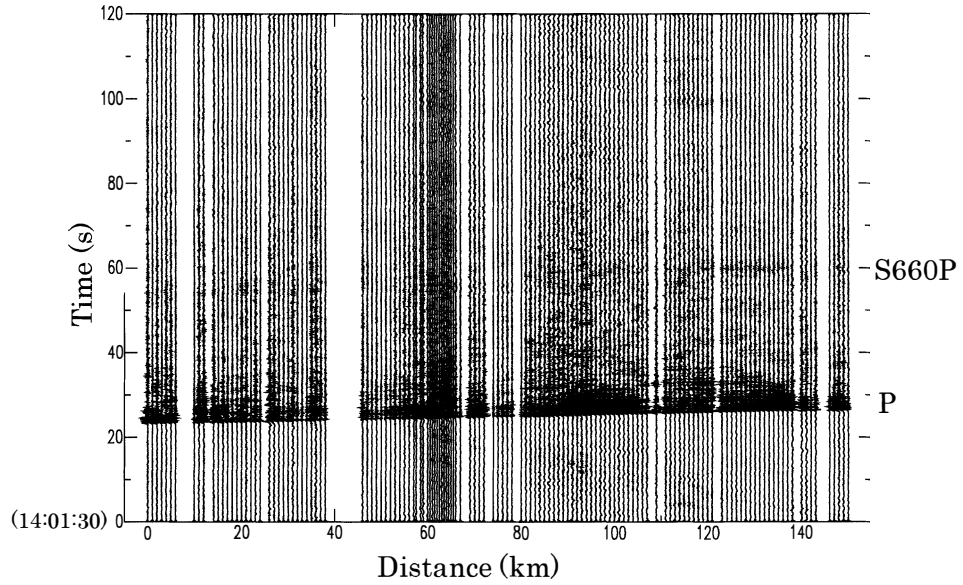

Fig. 3. Record section showing seismic waves of the Kermadec Is. event (m_b=4.5, depth=437 km). The vertical axis indicates relative time measured from Jan. 21, 2002, 1401:30.0 (UTC). We show here the original (no filter) traces with high signal-to-noise ratio. Signals during 20–30 s are composed of direct P and possibly reverberations in the ice sheet. Faint signals found in 50–60 s may be an S-P converted wave at the 660 km discontinuity just beneath the event (S660P).

in the earth's mantle. We find another arrival of phase about 30 s after the first arrival. This phase has almost the same slowness as that of the direct *P*. Thus the origin of this phase is presumably considered to be converted or reflected waves from discontinuity and/or heterogeneity located near the source. One possible explanation of this phase may be an S-P converted phases at the 660 km discontinuity (S660P) beneath the earthquake, because the travel time of S660P calculated by using IASP91 (Kennett and Engdahl, 1991) can explain this arrival. This phase is very important to determine the structure of the 660 km discontinuity and this clear recording shows the high quality of the seismological data obtained by the JARE-43 observation.

2.2. Icequakes

Figure 4 shows recordings of two icequakes. Two obvious phases between 10 and 70 s run from the northern side of the observation line (right hand side of Fig. 4), although the accurate direction of the incoming waves cannot be determined due to the line setting of the seismographs. Considering the similarity of the lengths of wave trains and the difference in slowness, these two phases may be a set of either *P* and *S* waves or direct and reflected waves from an icequake. In Fig. 4, two later phases with small amplitudes can be seen in time windows between 80 and 120 s. Considering the positive slowness, these two phases may be a set of waves from another icequake from the southern side of the observation line.

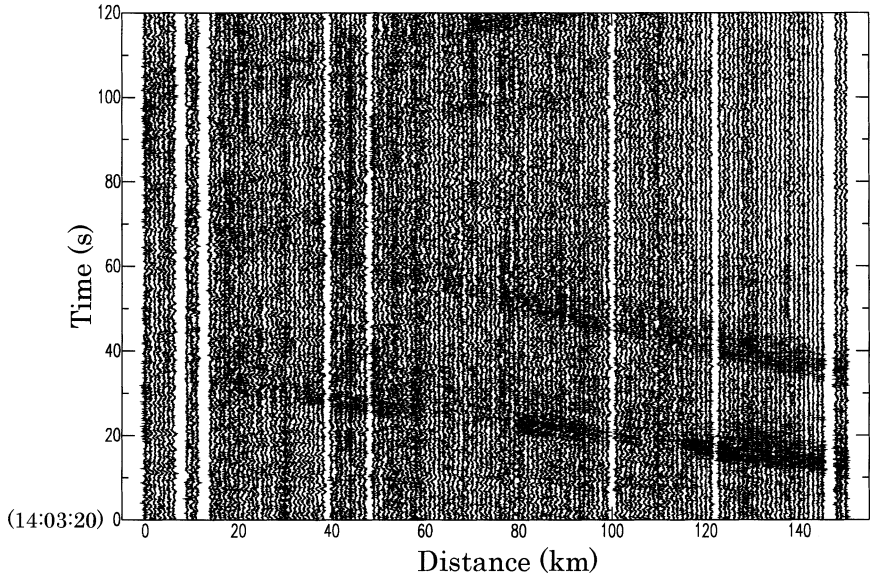

Fig. 4. Same as in Fig. 3 but for icequakes. The vertical axis starts from Jan. 14, 2002, 1403:20.0 (UTC).

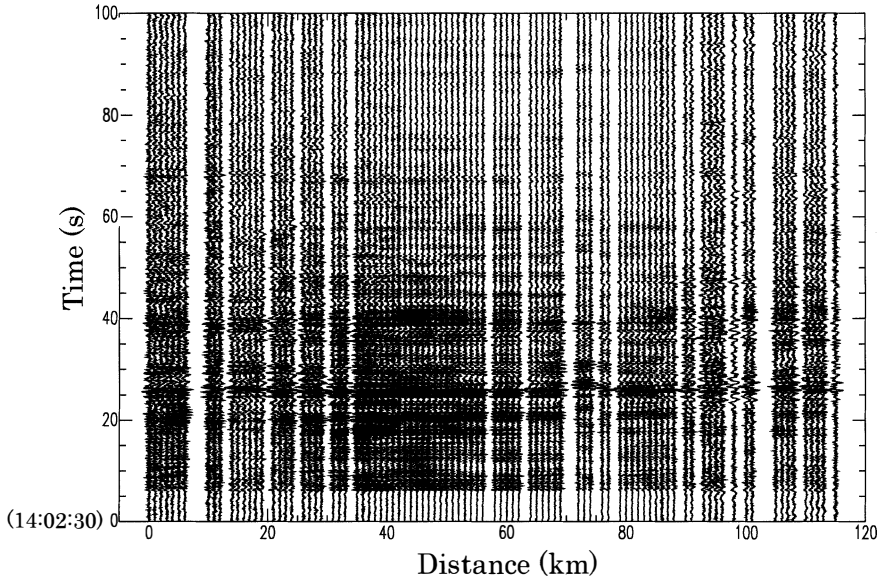

Fig. 5. Same as in Fig. 3 but for X-phases. The vertical axis starts from Jan. 27, 2002, 1402:30.0 (UTC).

These four signals traversing the observation line may have common features: (1) high-frequency components that are comparable with those of background noise, (2) relatively large slowness and (3) large fluctuation of amplitudes and weak correlation of the waveforms along the line. These characteristics support an inference that local icequakes occurred near the observation line.

2.3. X-phases

The third example of the recordings (Fig. 5) seems to be very strange (hereafter referred to as *X*-phases). Continuous arrivals of coherent signals are observed for a long duration about 100 s. This coherency is the same as observed in the teleseismic recording (Fig. 3). Slownesses of these signals are almost zero, which implies that these signals came from a direction perpendicular to the observation line. These features may indicate that these signals have the same sources as the teleseismic event. Referring to the worldwide earthquake catalogs (ISC bulletin and USGS PDE listings), a candidate for the event might be the Rat Is. (Aleutians) earthquake which occurred on Jan. 27, 2002, at 1342:44.4 (UTC). However, we will show in a later chapter that this event is probably not the source of the *X*-phases.

Though the sources of these signals are so far uncertain, we can find another

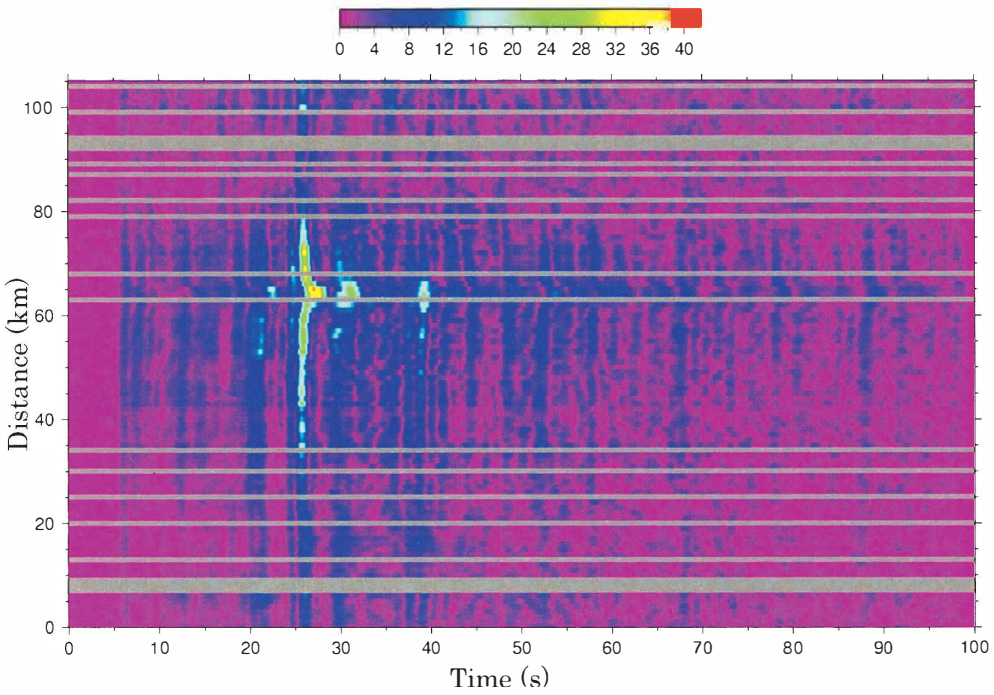

Fig. 6. Contour map showing envelope amplitudes of band-pass (1.0–2.0 Hz) filtered traces of the X-phases in Fig. 5. Traces with low signal-to-noise ratios are not used here and are colored in gray. Since the traces here are band-pass filtered, the number of traces with high signal-to-noise ratio is different from that in Fig. 5. Color scale is arbitrarily set to see an apparent amplitude variation within the map; scales in Figs. 7b–12 are colored in the same way.

interesting feature. Figure 6 shows the spatiotemporal variations of envelope amplitudes of band-pass filtered (1.0–2.0 Hz) seismograms. A remarkable feature is a time delay of the signal arrivals at around 65 km (at about 27, 31, 41, 45, 53 s and so on) compared with the corresponding arrivals found at other locations on the observation line. Moreover, arrivals at about 27 and 31 s show large amplitudes at 65 km with a time delay of about 1 s. This is not seen in other frequency bands and is also not found in the teleseismic recordings of Fig. 3. The distance of 65 km is located just above the valley structure of the bedrock (Fig. 2).

3. Analyses

The overview of the observed signals described in the previous section indicates the differences in (1) coherency of signals and (2) amplitude fluctuations along the line. We have performed two analyses by means of the stacking method and the running spectra method to estimate the above two differences.

First, we use phase-weighted stacking (PWS), developed by Shimmel and Paulssen (1997), instead of usual linear stacking. PWS is a kind of non-linear stacking. Each data point of a linearly stacked trace is weighted with an absolute value of an average of a sum of instantaneous phases of each trace. Thus, coherent signals through a seismological network can be constructively stacked and incoherent signals, even if some waveforms have larger amplitudes, result in a stacked signal with small amplitude due to the destructive sum of phase components. The stacking is performed by changing the slowness with the scanning interval of 0.001 s/km. We measure the slowness along the observation line.

Second, the running spectra are taken by applying the FFT to a 2 s windowed waveform (both sides of the window are hanning-tapered) with a time interval of 1 s. Before taking the spectrum, instrumental response is deconvolved from the original waveform.

3.1. Kermadec Is. event

Figure 7 shows the procedure of the PWS applied to teleseismic waves from the Kermadec Is. event. The traces in Fig. 7a are low-pass filtered with a cutoff of 2.0 Hz. A linearly stacked trace is obtained by searching for the slowness that maximizes the amplitude of the stacked direct *P*. All the traces are aligned on the direct *P* by taking the cross-correlation between each trace and the stacked *P* trace. This results in the alignment of the direct *P* on a line of zero slowness (Fig. 7a). The slowness here means a relative value compared with that of the direct *P*. Then we apply the PWS to the aligned traces by changing the slowness. The stacked traces are converted into envelopes by using the Hilbert transform and are plotted as a contour map (Fig. 7b).

In Fig. 7b, 6 successive peaks with an interval of about 0.8 s between 25–29 s are the direct *P*. Since an incident angle of the direct P is close to the vertical in case of this event, the interval of about 0.8 s can be interpreted as a two-way travel time within the ice sheet. Therefore, five peaks following the direct *P* may be reverberations within the ice sheet. The thickness of the ice sheet beneath this observation line is about 1.5 km (Fig. 2), which explains well the time intervals between the latter five peaks. The

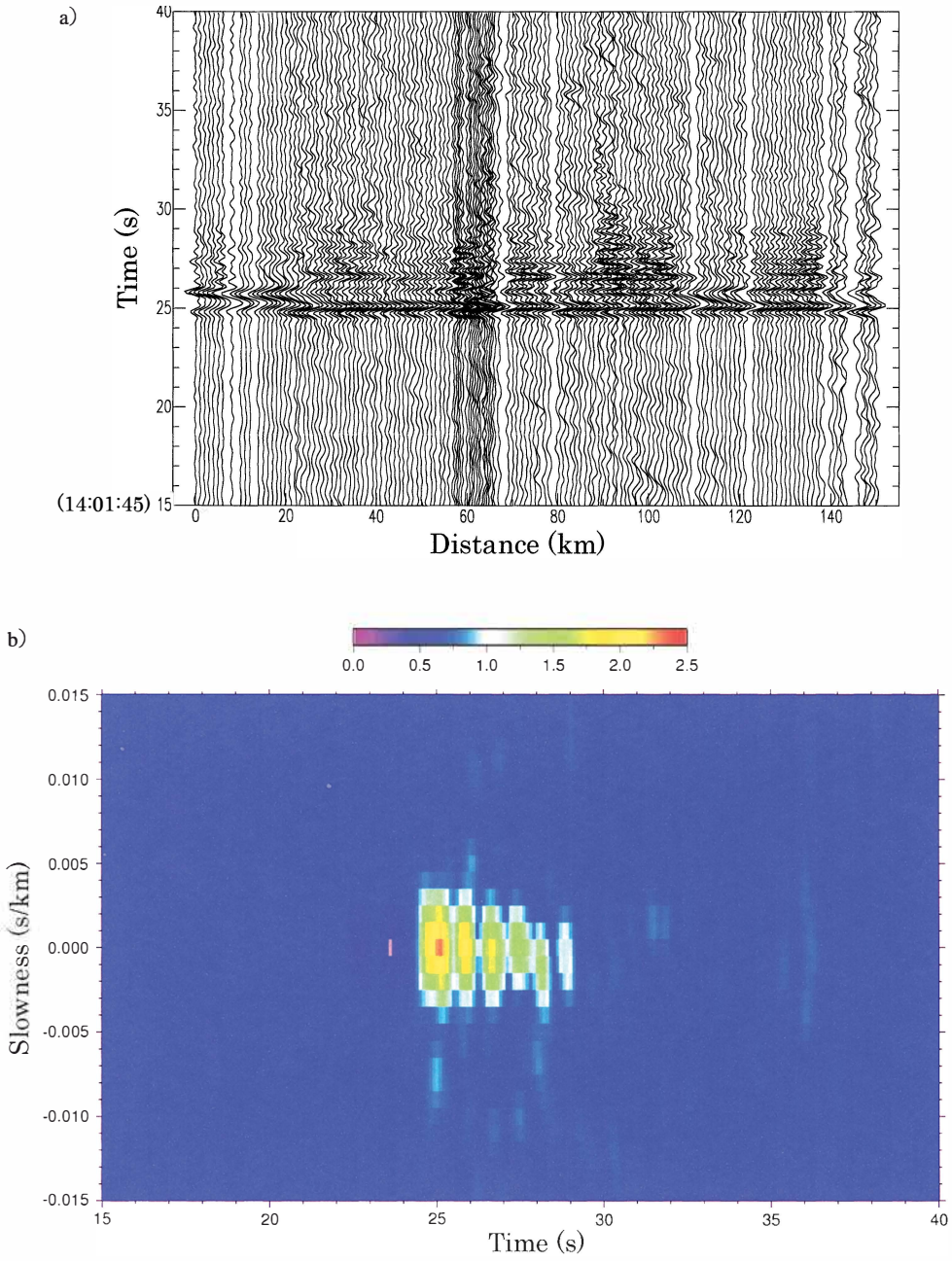

Fig. 7. (a) Traces of Kermadec Is. event, which are aligned on the onset of the direct P and are low-pass (2.0 Hz) filtered. The number of traces with high signal-to-noise ratio is different from that in Fig. 3. The pivot station is located at 74 km. The time window containing the direct P and the core-reflected PcP is shown here. (b) Contour map of PWS applied to the traces in (a).

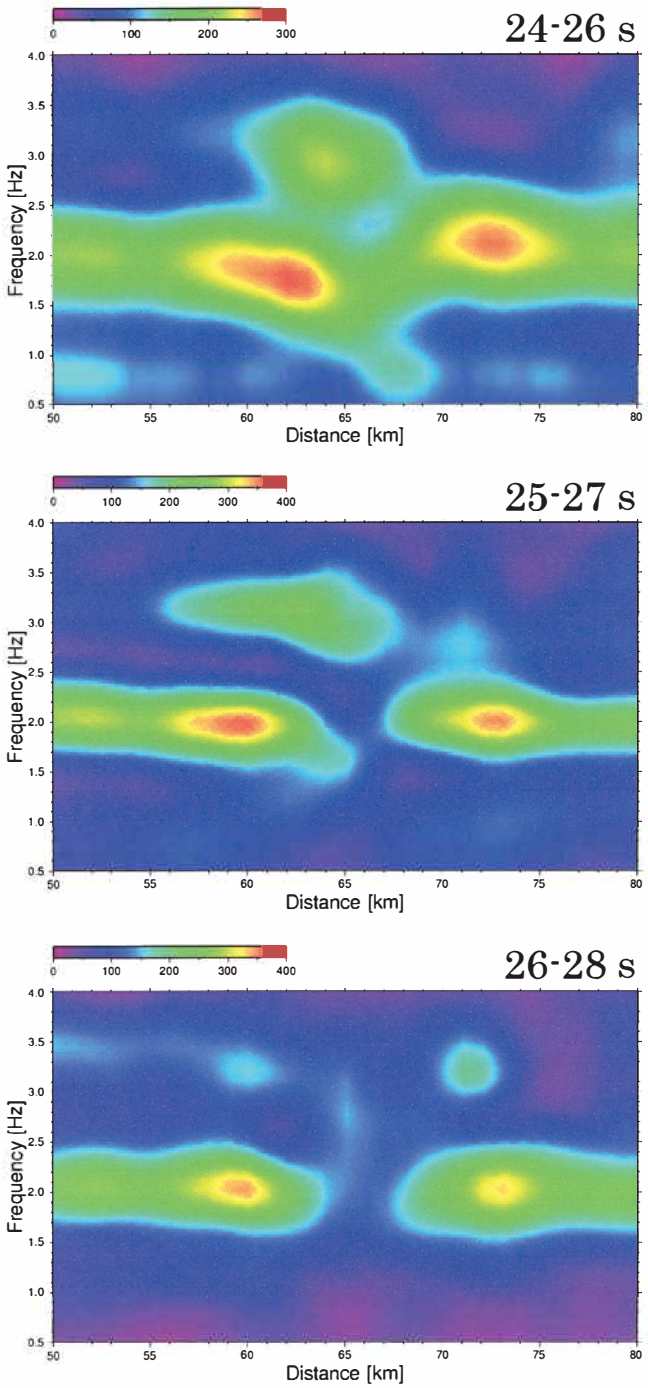

Fig. 8. Contour maps showing amplitudes of seismic energies plotted in the frequency-distance domain for traces of the Kermadec Is. event. Spectra are taken from the traces aligned on the direct P. Time windows are shown at the upper right of each plot.

source time function of this event is not known. However, a deep focus event with small magnitude has a simple source time function, and these peaks can be caused by the reverberations rather than complexity of the source. All the peaks have almost the same slowness as that of the direct *P*.

The core-reflected *PcP* is detected at (36 s, 0.0 s/km). Note that the theoretical relative slowness measured along the great-circle path between the event and the stations is about −0.01 s/km. The back azimuth from the center of the observation line is 143.3°, which is almost normal to the strike of the observation line. Therefore the relative slowness of the *PcP* measured along the observation line would be almost the same as that of the direct *P*.

Figure 8 shows the running spectra of three different time windows. The figure shows that the dominant frequency in these windows is about 2.0 Hz. Of greatest interest is the clear gap of high energy of 2.0 Hz at about 65 km where the valley structure exists (Fig. 2). The stations on both sides of this gap (at around 59 km and 72 km) receive higher energies. We can also see the peaks at frequency about 3.0 Hz in the middle of the observation line.

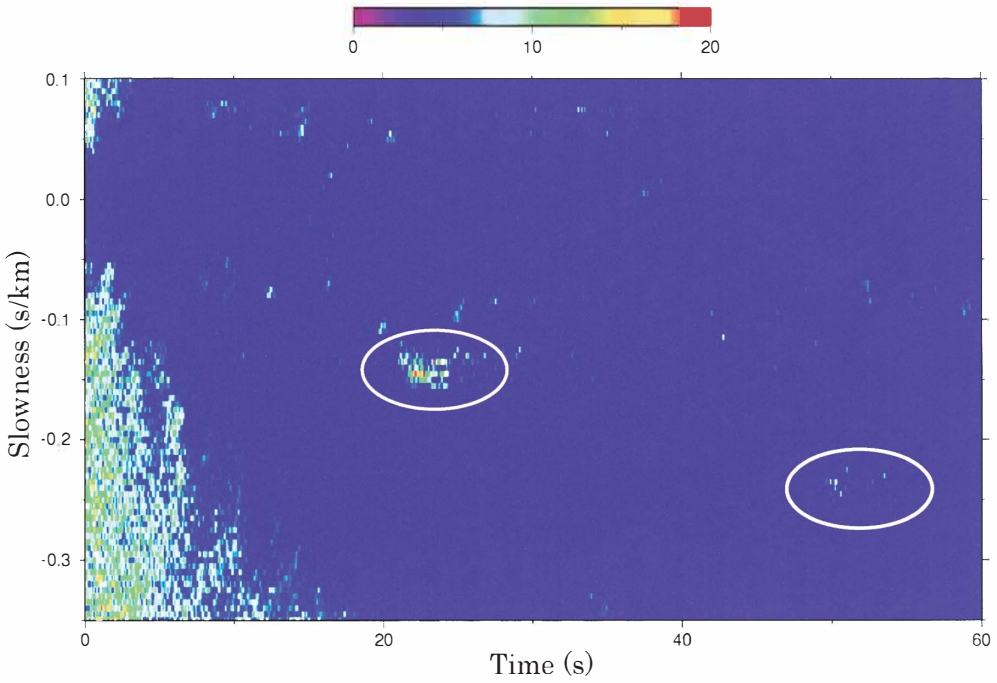

Fig. 9. Same as in Fig. 7b but for icequakes. Peaks corresponding to two obvious waves shown in Fig. 4 are indicated by white ellipses: peaks at (23 s, −0.135 s/km) and (51 s, −0.235 s/km). Note that high amplitudes found at the upper and lower left are artifacts caused by the PWS applied to zero-amplitude portions: since the zero amplitudes have the same value of phase components, a sum of the phase components should have a large value.

3.2. *Icequakes*

The PWS contours of the icequakes are shown in Fig. 9. Because of the incoherency of these icequakes, alignment on arrival cannot be done as above. Thus the vertical axis in Fig. 9 indicates the absolute slowness. Two peaks corresponding to the icequakes in Fig. 4 are seen at (23 s, −0.135 s/km) and (51 s, −0.235 s/km). Compared with peaks in Fig. 7b, those in Fig. 9 are weak and scattered. Since the PWS enhances the signal that is coherent through the network, we can find that the waves

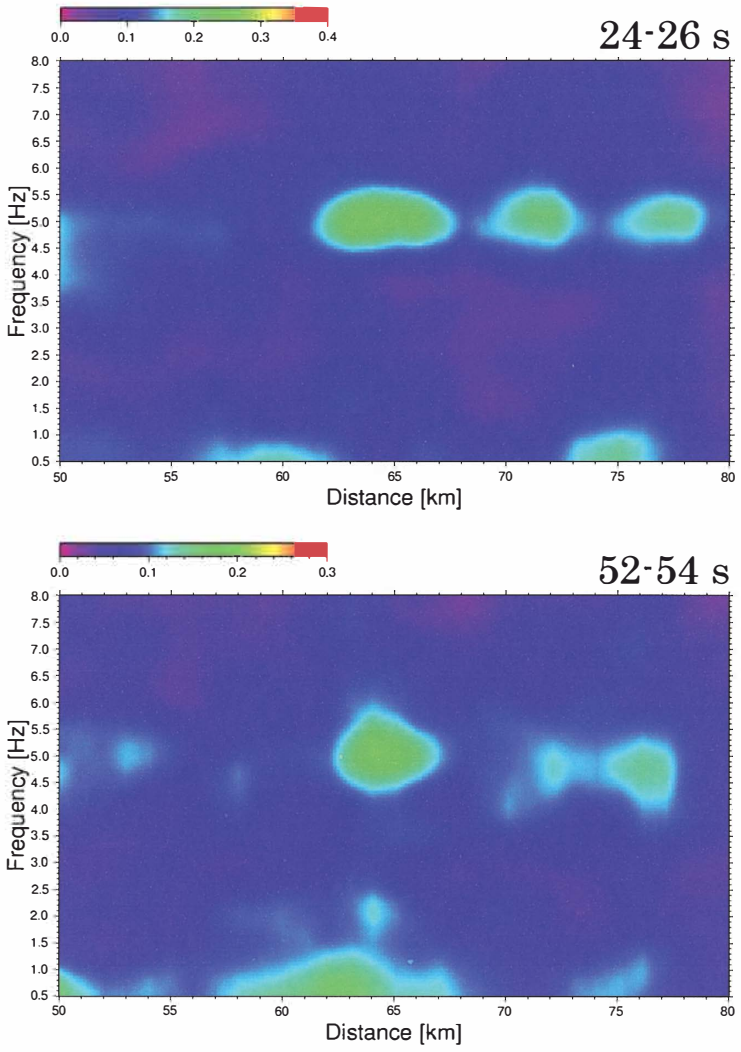

Fig. 10. Same as in Fig. 8 but for icequakes. Contours of top and bottom correspond to the two obvious waves shown in Figs. 4 and 9. Note that the spectra are taken in the time windows of the traces that are time-shifted by using the best slownesses of two waves found in Fig. 9. The pivot station is located at 74 km. Thus time windows shown at the upper right of each plot indicate those of the pivot trace.

generated by the icequakes are not coherent and show large fluctuations of the waveforms in the distance range of about 100 km.

The running spectra of the icequakes are indicated in Fig. 10. In this case, the dominant frequency is about 5.0 Hz and a peak is located at 65 km where we find the clear gap of 2.0 Hz in the Kermadec Is. event (Fig. 8).

3.3. X-phases

Figure 11 shows the PWS stacking of the *X*-phases (Fig. 5). As in the case of the Kermadec Is. event, we use the relative slowness with respect to the first arrival of the *X*-phases. Consecutive arrivals with high coherency are found for about 100 s after the onset. This long duration is not found in the cases of either the Kermadec Is. event or icequakes. Slownesses of all the arrivals are almost the same. This implies that these wave energies reach the observation line with the same incident angle and azimuthal direction.

The dominant frequency of the *X*-phases is 2.0 Hz, as in the Kermadec Is. event, as shown in the running spectra in Fig. 8. In addition to the gap of 2.0 Hz at about 65 km, we can see one strange feature in the spectra, which is not found in the Kermadec Is. event. In Fig. 12, this gap of 2.0 Hz at 65 km turns into a peak of 1.5 Hz with a delay of only one second (middle and bottom in Fig. 12). This peak of 1.5 Hz corresponds to the energy peak at (27 s, 65 km) in Fig. 6.

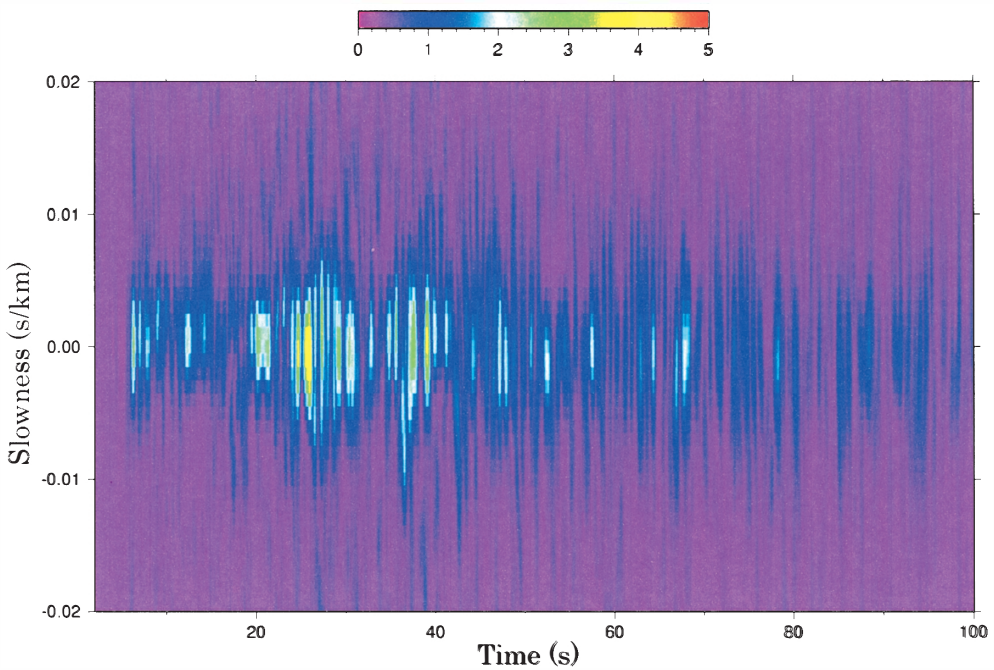

Fig. 11. Same as in Fig. 7 (b) but for the X-phases.

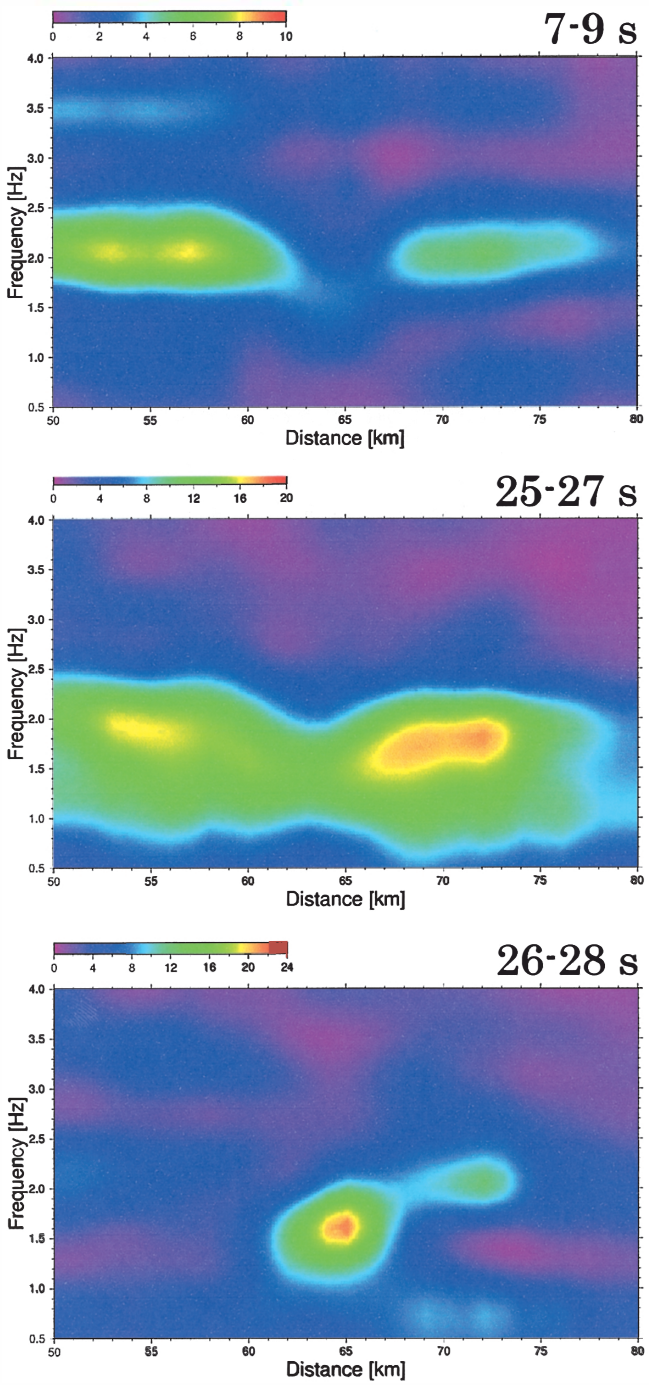

Fig. 12. Same as in Fig. 8 but for the X-phases. Top and middle panels show the gap of high energy of 2.0 Hz at around 65 km, and the bottom panel the peak of 1.5 Hz just a second late after the time window showing the gap in the middle panel.

4. Discussion

We shall try to explain two characteristic features found in the previous chapter: (1) the origin of the *X*-phases and (2) anomalous fluctuations of frequency components.

4.1. Origin of the X-phases

A significant feature of the *X*-phases is successive arrivals of seismic energies with almost zero slowness for about 100 s after the onset. One candidate for the causative event might be the Rat Is. (Aleutians) earthquake. However, we will show that it was not likely the event which produced the *X*-phases. The epicentral distance from the event to the center of the observation line is about 152°. Since this event has a small magnitude (4.8 m_b), it is uncertain that such a small earthquake could be recorded by seismographs at a large epicentral distance. Indeed, seismological networks in Japan, which were located at a distance of about 40° from the event, did not observe it. Moreover, seismic waves from this event recorded at the JARE observation line should be core-penetrating phases, such as of the PKP branches (df, bc, ab). Even if we take into account a set of phases composed of PKPs and depth phases (pPKP and sPKP), we cannot explain the successive arrivals of the *X*-phases.

Another reason why the *X*-phases may not be the PKP family comes from a comparison of the waveforms with the Kermadec Is. event. If we consider the *X*-phases to be the waves from the Rat Is. event, the back azimuth from the center of the observation line is 107.4° and the incident angle to the boundary between the ice sheet and the topmost crust ranges from 4.6° (PKPdf) to 13.4° (PKPab). They are 143.3° and 18.0° respectively for the direct *P* of the Kermadec Is. event. If we consider the ray paths of the PKPs of the RAT Is. event and the direct *P* of the Kermadec Is. event to a station on the observation line, the piercing points of these waves to the boundary differ horizontally by only a few hundred meters. This value may be much smaller than the horizontal scale length of the valley structure of about 10 km shown in Fig. 2. Therefore, we cannot expect that different responses would be generated by the complex topography of the boundary between the Rat Is. event and the Kermdec Is. event. However, there is a difference between the waves of the *X*-phases and the Kermadec Is. event. The gap of 2.0 Hz in the middle part of the seismic line is found in these two cases (Figs. 8 and 12). The peak of 1.5 Hz with a time delay of about a second after the gap is seen only in the *X*-phases (Fig. 12, lower part) and that of 3.0 Hz without time delay is only seen in the Kermadec Is. event. Thus this difference may lead to a conclusion that the *X*-phases would not be able to be the waves of the Rat Is. event.

The features of the *X*-phases are clearly different from those of the local icequakes (Figs. 4 and 5). A possibility of the origin of the *X*-phases may be regional intraplate earthquakes. Such regional events around Antarctica from 1900 to 1999 have been compiled by Reading (2002). East Antarctica from 90° E to 180° E, in particular the Wilkes Land, Transantarctic Mountains and Ross Sea areas, is the region showing the highest seismicity in Antarctica. Figure 13 compares the stacked trace of the *X*-phases with the observed broadband trace at SYO (Syowa Station). Although it seems to be difficult to compare the arrivals between these two traces, the maximum amplitudes of seismic phases appear to arrive at SYO with the delay of several seconds. Therefore the

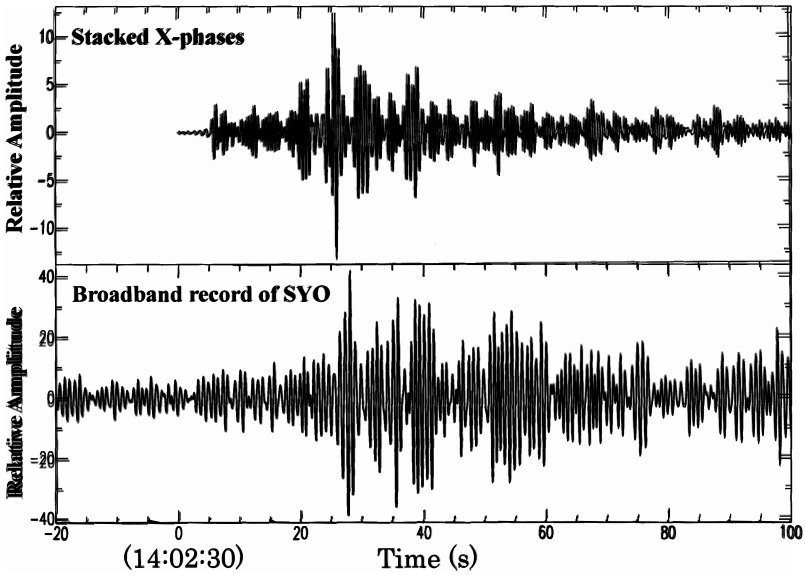

Fig. 13. Comparing the stacked trace of the X-phases (top) and a broadband record of SYO (bottom) after correction of the instrument response of the seismograph used in the JARE-43 experiments. Both traces are band-pass (1.0–2.0 Hz) filtered. The origin of the time axis (0 s) corresponds to 1402:30.0 (UTC).

X-phases may be considered to come to the observation line and SYO from the relatively active seismogenic region in the Wilkes Land–Ross Sea area.

4.2. Gap and peak in the spectra

Abrupt change of the frequency spectra in the recordings was observed at the stations at around 65 km just above the valley topography at the interface between the ice sheet and the topmost crust. An anomaly in the observed waves changes from local to teleseismic waves, although the origin of the *X*-phases is uncertain. The anomaly, which is commonly found in the three types of events, should be associated with the valley structure, not with the heterogeneous structure around the source region and/or the complexity of the source mechanism. A concave structure focuses seismic waves on the surface (*e.g.* Aki and Richards, 1980). In this case, adding to the focusing of waves with frequencies of 1.5, 3.0 and 5.0 Hz, defocusing of 2.0 Hz was observed (Figs. 8, 10 and 12). This frequency dependence of the focusing and defocusing of the seismic waves may be caused by not only the valley structure but also the short distance between the valley structure and the surface, that is, variations of thickness of the ice sheet. The average thickness of the ice sheet beneath the observation line is about 1.5 km, which is shorter than or comparable to the wavelength of the seismic waves used in this study (1.5 Hz–5.0 Hz). Thus, we can expect complex interference of the incident waves by the valley structure.

An other interesting phenomenon is found in Fig. 6. In addition to the delay of

the arrivals at around 65 km described in Section 2.3, we find, by close inspection, a small arrival without delay just before the late arrival, at about 25 s. Such normal arrivals are also found at 6 s (onset) and 35–40 s, respectively. The *X*-phases consist of normal and delayed arrivals. It is clear from the recording of the Kermadec Is. event that the *P*-wave arrivals are not delayed at about 65 km. Thus, the normal arrivals of the *X*-phases may be the *P* wave, but the delayed arrivals might not be the *P* wave. One possibility is *S*-wave arrivals. Whether the *S*-wave arrival is delayed at around 65 km would be clarified by the data of the *S*-wave arrivals of the Kermadec Is. event. Unfortunately, the *S*-wave arrivals were out of range of the recording period. If the above hypothesis is valid, it is possible that the origin of the *X*-phases was not a teleseismic event but a regional event, because the *S*-wave arrivals from a teleseismic event are out of range of the recordings.

5. Conclusions

The seismic recordings of natural sources obtained from JARE-43 seismic exploration provide evidence of interesting features of the wavefield. We find discordances of the frequency spectra and of the arrival times in the traces. The following anomalous features are seen in the waveforms of the stations just above the valley structure at the boundary between the ice sheet and the upper crust. (1) The frequency components of 1.5, 3.0 and 5.0 Hz are large compared with those at other stations, while those of 2.0 Hz are small. (2) A difference of the response generated from the valley structure might exist according to whether incident waves are *P* or *S* waves: *P*-wave incidence to this valley structure might result in normal arrival; on the other hand, *S*-wave arrival might be delayed.

As is evident in the teleseismic records (Kermadec Is. event), the high signal-to-noise ratio of the records indicates that the JARE-43 data are useful to study not only local shallow structure but also deep structure within the Earth.

Acknowledgments

The authors gratefully acknowledge all the participants of the JARE-42 and JARE-43 for their great effort to perform the seismological survey on the Mizuho Plateau. Great thanks, especially, are due to Drs. H. Miyamachi, S. Toda and T. Matsushima for their management of the experiments. The authors also thank Dr. I. Nakanishi and an anonymous reviewer for valuable comments and extremely detailed reviews. Parts of the figures have been prepared with generic mapping tools (GMT) (Wessel and Smith, 1995).

References

Aki, K. and Richards, P.G. (1980): Quantitative Seismology. Freeman, New York, 759–766.

Kanao, M. (2001): Crustal evolution and deep structure viewed from East Antarctic Shield, "Structure and Evolution of the East Antarctic Lithosphere 'Geotransect Project'"—Outline and scientific significance—. Bull. Earthq. Res. Inst., Univ. Tokyo, **76**, 3–12.

Kapitsa, A.P., Ridley, J.K., Robin, G. de Q., Siegert, M.J. and Zotikov, I.A. (1996): A large deep freshwater lake beneath the ice of central East Antarctica. Nature, **381**, 684–686.

Kennett, B.L.N. and Engdahl, E.R. (1991): Travel times for global earthquake location and phase identification. Geophys. J. Int., **105**, 429–465.

Mae, S. (1978): The bedrock topography deduced from multiple radar echoes observed in the Mizuho Plateau, East Antarctica. Nankyoku Shiryô (Antarct. Rec.), **61**, 23–31 (in Japanese with English abstract).

Miyamachi, H., Murakami, H., Tsutsui, T., Toda, S., Minta, T. and Yanagisawa, M. (2001): A seismic refraction experiment in 2000 on the Mizuho Plateau, East Antarctica (JARE-41)—Outline of observations—. Nankyoku Shiryô (Antarct. Rec.), **45**, 101–147 (in Japanese with English abstract).

Miyamachi, H., Toda, S., Matsushima, T., Takada, M., Takahashi, Y., Kamiya, D., Watanabe, A., Yamashita, M. and Yanagisawa, M. (2003a): A seismic refraction and wide-angle reflection exploration in 2002 on the Mizuho Plateau, East Antarctica—Outline of observations (JARE-43)—. Nankyoku Shiryô (Antarct. Rec.), **47**, 32–71 (in Japanese with English abstract).

Miyamachi, H., Toda, S., Matsushima, T., Takada, M., Watanabe, A., Yamashita, M. and Kanao, M. (2003b): Seismic refraction and wide-angle reflection exploration by JARE-43 on Mizuho Plateau, East Antarctica. Polar Geosci., **16**, 1–21.

Reading, A.M. (2002): Antarctic seismicity and neotectonics. R. Soc. N.Z. Bull., **35**, 479–484.

Shimmel, M. and Paulssen, H. (1997): Noise reduction and detection of weak, coherent signals through phase-weighted stacks. Geophys. J. Int., **130**, 497–505.

Siegert, M.J., Ellis-Evans, J.C., Tranter, M., Mayer, C., Petit, J.-R., Salamatin, A. and Priscu, J.C. (2001): Physical, chemical and biological processes in Lake Vostok and other Antarctic subglacial lakes. Nature, **414**, 603–609.

Takada, M., Toda, S., Kamiya, D., Matsushima, T. and Miyamachi, H. (2003): Radio echo sounding survey along the profile of the JARE-43 seismic exploration on the Mizuho Plateau, East Antarctica. Nankyoku Shiryô (Antarct. Rec.), **47**, 380–394 (in Japanese with English abstract).

Tsutsui, T., Murakami, H., Miyamachi, H., Toda, S. and Kanao, M. (2001): *P*-wave velocity structure of the ice sheet and the shallow crust beneath the Mizuho traverse route, East Antarctica, from seismic refraction analysis. Polar Geosci., **14**, 195–211.

Wessel, P. and Smith, W.H.F. (1995): New version of the generic mapping tools released. EOS Trans. AGU, **76**, 329.